Forbidden Radical Rearrangements. Comparison with Potential Surfaces of Jahn–Teller Radicals

Peter Bischof

Contribution from the Institut für Organische Chemie der Technischen Hochschule Darmstadt, D 61 Darmstadt, West Germany. *Received March 2, 1977*

Abstract: The MINDO/3-UHF method has been used to investigate the potential surface behavior of some doublet systems. The calculations support the expected strong similarity between the transition states of forbidden electrocyclic radical rearrangements and the ground state of Jahn-Teller distorted radicals. Comparisons of $4n + 1$ with $4n + 3$ electron π radicals show that there is no simple rule to determine their relative stabilities.

The stereochemistry of a reaction involving closed shell reactants can be predicted using the Woodward–Hoffmann rules.[1] In this framework, a considered reaction path is either "forbidden" or "allowed" depending on whether or not the highest occupied molecular orbital (HOMO) and the lowest unoccupied molecular orbital (LUMO) become accidentally[2] degenerate along the reaction coordinate. It should be emphasized that the term "forbidden" is not spectroscopically strict: it simply implies that there is most likely another—allowed—reaction path that involves less activation energy and thus dominates the process. Such differences of activation energies have typically been estimated to be in the order of 15–30 kcal/mol,[3] a magnitude large enough to determine the stereochemistry of most reactions.

For reactions involving radicals, the situation is not as clear cut.[4] The corresponding difference in activation energy is expected to be much smaller and may easily be overruled by other effects. In contrast to closed shell systems, there are *three* principally different types of frontier orbital correlations to be considered. This is illustrated in Figure 1. The highest occupied molecular orbital (HOMO) of the system is (in its dominant ground state configuration) simply occupied. Along the reaction coordinate λ, it is possible that the HOMO "crosses" the lowest unoccupied molecular orbital (LUMO; case A), the highest doubly occupied molecular orbital (case B), or that it remains the HOMO throughout (case C). In this scheme, the disrotatory ring opening of the cyclopropyl radical would be an example of case A, while in the conrotatory mode it would follow case B. As an example for case C, the conrotatory benzocyclobutene/*o*-quinodimethane anion rearrangement has been discussed recently.[5]

According to the Woodward–Hoffmann rules, cases A and B represent "forbidden" reaction paths, since the ground state configuration of the reactant correlates with one of two different excited configurations of the product.

Simple HMO considerations reveal that most radical rearrangements (and electrocyclic ring openings in particular) must proceed via one of the forbidden reaction paths A or B.[4] Therefore, it will be most important to find out which one of the corresponding transition states is more stable. Although many attempts have been made to provide simple rules for estimating their relative energies, no generally valid conclusions were reached so far.

General Considerations

A rearrangement of a molecule or a radical consisting of N nuclei can be regarded as a transformation of a vector in a $3N - 6$ dimensional space, where the elements of the vector are the intramolecular nuclear displacements. Considering conrotatory and disrotatory ring openings, it has been adopted[1] to assume one element of symmetry R: a twofold axis C_2 or a mirror plane C_s, respectively. Under these circumstances, any displacement Q_i is either symmetrical, antisymmetrical, or a superposition of such displacements. The displacements will here be called "dynamic modes" in order to distinguish them from the vibrational modes which are normally considered to be orthogonal.

Note that a symmetrical dynamic mode does not alter the symmetry of the molecule, while an antisymmetrical dynamic mode in general leads to a system of C_1 symmetry, provided that R is the only symmetry element. However, this general description of a reaction is seldom used in practice. To compute a "reaction profile", the chemist choses a single specific reaction coordinate Q_1, mostly a symmetrical dynamic mode such as the length of the bond being broken in the process.

At this point, it will be useful to illustrate an important difference between the state correlation diagrams of a forbidden closed shell reaction and a forbidden open shell reaction. While the former type of reactions has been studied extensively,[6] we shall focus mainly on the latter. For the following discussion it shall be assumed that the reaction coordinate Q_1 is a symmetrical mode as indicated above.

Hence, the relevant symmetry element R (the C_2 axis for a controtatory, the plane of symmetry σ for a disrotatory process) is retained. Under this condition, the mentioned point X will be reached, at which the frontier orbitals do cross.

It should be kept in mind that in this picture the Born–Oppenheimer approximation breaks down at this point X, since the single configuration electronic wave function is strongly dependent upon the nuclear positions. However, we shall not consider this complication any further, since this actual situation will never occur for the reasons given later.

For a system with an even number of electrons (i.e., for a "closed shell reaction"), there are evidently three singlet configurations which at the point X have about the same energy. Two of these are symmetrical, the third one antisymmetrical with respect to R. This is a simple consequence of the fact that the two crossing orbitals must have different symmetries. Owing to the degeneracy of these configurations, the (symmetrical) ground state of the molecule can no longer be represented by a single Slater determinant: configuration interaction will prevent the crossing of the state potential surfaces.[1,7]

However, in case of a system with an odd number of electrons (i.e., an "open shell reaction"), there are only two doublet configurations of comparable energy, one of which is the singly excited configuration of the other and vice versa. Since the configurations have different electronic symmetries, they do not interact and the state potential surfaces indeed may cross.[7] The resemblance of this situation with that of a Jahn–Teller

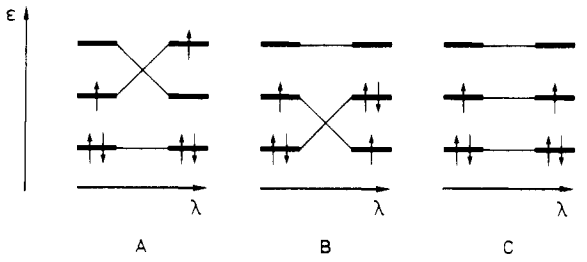

Figure 1. The three possible frontier orbital correlation diagrams of reactions involving reactants with an odd number of electrons.

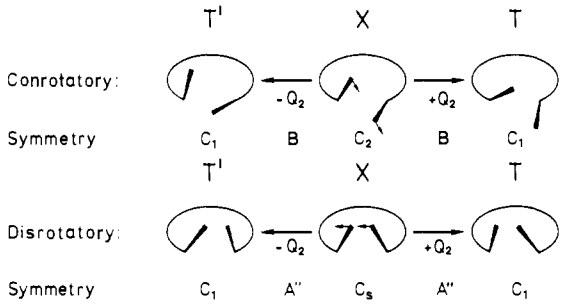

Figure 3. Effect of an antisymmetric distortion mode Q_2 upon a symmetric structure X leading to the unsymmetrical structures T and T'.

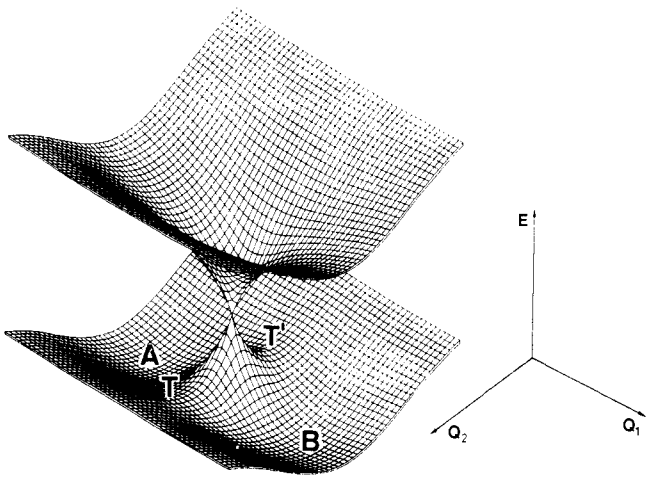

Figure 2. Qualitative potential surface behavior for a forbidden open shell reaction. Point X (see text) corresponds to the tip of the double cone.

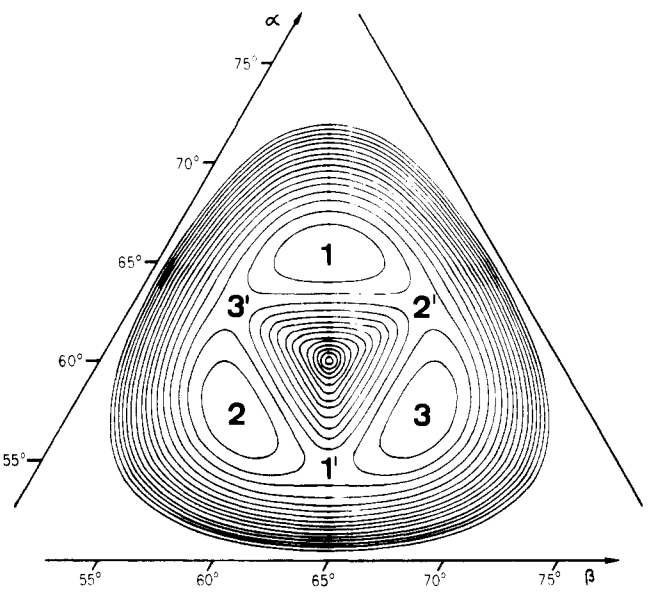

Figure 4. Potential surface of the cyclopropenyl radical (C_3H_3·) as a function of the three CCC angles α, β, and γ.

state radical therefore becomes evident: the system will be stabilized by lowering of its symmetry.

From these arguments, we expect the qualitative behavior of the state potential surfaces shown in Figure 2. In this plot, Q_1 represents the reaction coordinate symmetrical with respect to R, while Q_2 is an antisymmetrical mode. Q_2 may be termed the Jahn-Teller distortion mode. Purely qualitative considerations lead to the following conclusions: (a) Since Q_1 is a symmetrical dynamic mode, the complete potential surface is symmetrical with respect to this coordinate. (b) If R is a C_2 axis (conrotatory process), T and T' have the same structures, if R is a mirror plane (disrotatory process), T and T' are enantiomer transition states. This is indicated in Figure 3.

Although these qualitative arguments illustrate quite nicely the close similarity between the electronic structures of Jahn-Teller state radicals and the transition states of "forbidden" radical rearrangements, they do not lead to usable predictive conclusions concerning which of the two forbidden reaction paths (the earlier mentioned case A or case B) will be "less forbidden" and thus dominate the reaction.

For this purpose, more detailed calculations are necessary. We wish to demonstrate that the MINDO/3-UHF[8] method seems to be an adequate "experimental tool" in this sense. Specifically, this model seems to describe Jahn-Teller potential surfaces very well.

As anticipated above, we will have to consider two types of systems that contain two partially filled degenerate orbitals: (a) filled with one electron (case A) and (b) filled with three electrons (case B). Compared with the isoelectronic cyclic Hückel perimeters, the former corresponds to the $4n + 3$ electron system, while the latter is a $4n + 1$ electron radical.

Jahn-Teller State Radicals

The most simple case of a $4n + 3$ π radical ($n = 0$) is the cyclopropenyl radical. Since this molecule is a key case in this connection, we will outline our results in further detail.

Simple HMO arguments show that the singly occupied degenerate π orbital of the molecule will give rise to a Jahn-Teller distortion to yield either an acute-angled (**1'**) or an obtuse-angled triangle (**1**) depending on whether the symmetric e_S or the antisymmetric e_A orbital is occupied by the unpaired electron. The optimized structures (enforcing C_{2v} symmetry) using MINDO/3-UHF[8] are shown in Figure 6.

Our results are on line with recently published theoretical predictions[9] that both structures are points on *one common* potential surface and that only **1** corresponds to a true minimum, while **1'** is unstable with respect to a distortion of B_2 symmetry leading to two equivalent structures of type **1**. Zahradnik[9] found the opposite relative stabilities of **1** and **1'**. Some ab initio calculations[10] support our result, while others[11] are contradictive.

We have calculated the ground potential surface of cyclic $(CH)_3^+$ as a function of the CCC angles, optimizing the remaining ten geometrical variables without any restrictions. The result is shown in Figure 4, where the calculated heat of formation is plotted as a function of α and β. The distance between the equipotential lines is 0.2 kcal/mol. In this plot, the three minima **1**, **2**, and **3** are the three equivalent $^2A_2$ structures, while **1'**, **2'**, and **3'** are the $^2B_1$ saddle points.

Our structures **1**, **2**, and **3** interconvert with a calculated barrier of 0.5 kcal/mol. Günthard et al.[12] have established an

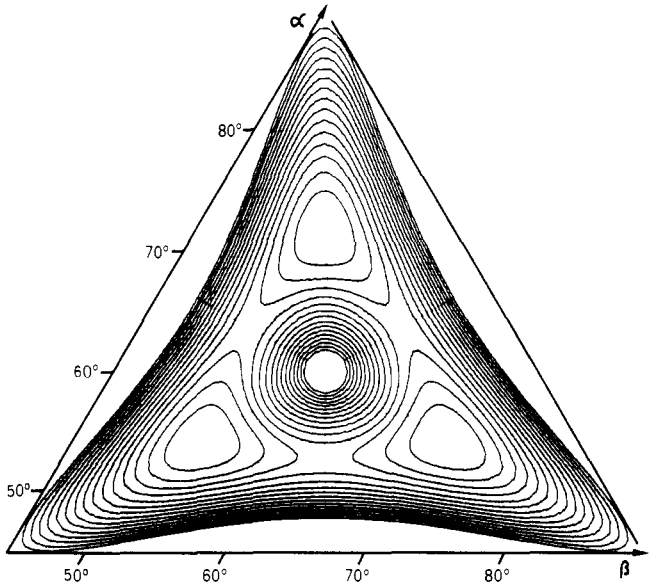

Figure 5. Potential surface of the cyclopropyl radical cation ($C_3H_6^+$) as a function of the three CCC angles α, β, and γ.

experimental value of 0.57 kcal/mol. Hence, our prediction is in perfect agreement with experiment.

Two additional interesting features were found in this calculation: at any point of the potential surface, the radical was calculated to be planar within the convergence criteria. Furthermore, the "breathing" of the carbon framework was calculated to be essentially zero; the sum of the three carbon–carbon bond lengths remained constant at 4.21 Å, although the bond alternation is quite considerable.

The parallelism of this potential surface with the one shown in Figure 2 can be illustrated in further detail. Considering the "reaction" of **1′** to yield **1**, the reaction coordinate Q_1 would be the straight line connecting both points: the C_{2v} symmetry of the "reactant" is maintained. The crossing point X now is the structure corresponding to D_{3h} symmetry of the radical, where the former $^2B_1$ ground state configuration suddenly switches to $^2A_2$ symmetry. This symmetry-forbidden "reaction path" is accompanied by a high activation energy, while the two alternative "real" reaction paths **1′ → 2 → 3′ → 1** and **1′ → 3 → 2′ → 1** only need the mentioned 0.5 kcal/mol activation energy.

We shall now investigate a radical in which the degenerate orbital is occupied with three electrons; a $4n + 1$ radical in comparison with isoelectronic Hückel systems. Unfortunately, the parent uncharged radical of this type (the cyclopentadienyl radical) cannot easily be illustrated in a two-dimensional plot. Radicals of this type, on the other hand, are quite commonly found in photoelectron spectroscopy. A convenient example is therefore provided by the ground state of the cyclopropane radical cation, in which the E orbital (HOMO) of the parent molecule has lost an electron in the first ionization process[13] and is known to suffer Jahn–Teller distortion. The ground state hypersurface of the generated ion has been investigated in some detail by semiempirical calculations.[14]

Again, we have calculated the complete potential surface as a function of the CCC angles of the ion, optimizing the remaining 19 variables with no restrictions. The result is shown in Figure 5. The distance between the equipotential lines is 0.4 kcal/mol. Apart from the even larger bond alternation the results strictly parallel those found for $(CH)_3^+$: only one Jahn–Teller isomer (the obtuse angled, $^2A_1$) is a real minimum, while the other (acute angled, $^2B_2$) is unstable toward a vibration of B_2 symmetry. The two structures are again shown below.

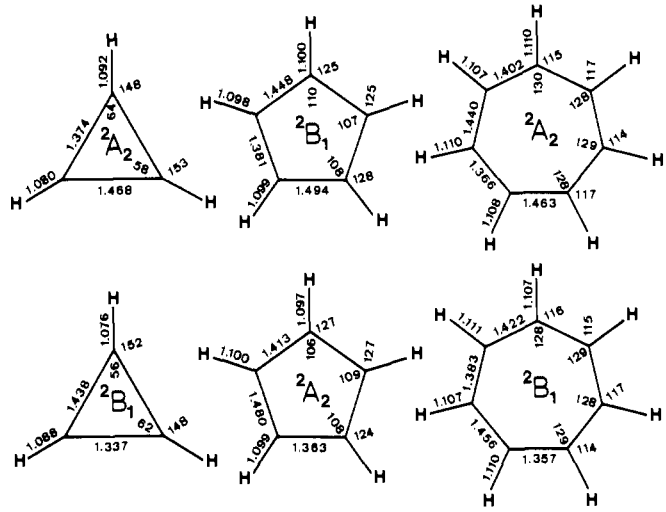

Figure 6. Calculated equilibrium structures (top) and saddle points (below) of cyclopropenyl, cyclopentadienyl, and tropyl radicals. All structures shown were predicted to have C_{2v} symmetry. (C_2 axis shown vertical.)

Table I. Heats of Formation (ΔH_f) and Barriers of Interconversion ($\Delta I^{\ddagger}$) of Cyclic π Radicals (kcal/mol)

R·	ΔH_f		$\Delta I^{\ddagger}$	
	Calcd	Exptl	Calcd	Exptl[a]
Cyclopropenyl	96.8		0.5	0.57[12]
Cyclopentadienyl	66.8	70 ± 5	0.1	0.14[20]
Tropyl	47.8	65[17]	0.0	0.0[22]

[a] The two decimal places given in the table arise from conversion of other energy units; they do not imply such accuracy.

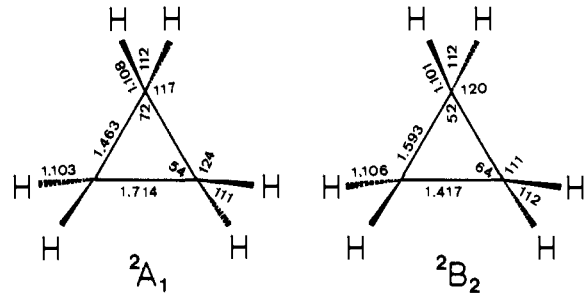

Note that $C_3H_6^+$ is not isoelectronic with $C_3H_3^{2-}$, since the electronic state symmetries of the former are $^2B_2$ and $^2A_1$, while the ones of the latter are $^2B_1$ and $^2A_2$, respectively.

The findings discussed above about $4n + 1$ and $4n + 3$ type radicals seem to be quite general. Calculations on the cyclopentadienyl radical as well as on the cycloheptatrienyl radical (the "tropyl" radical) also show that only one isomer corresponds to a true minimum, while the other is a saddle point. The barrier of interconversion from one of the equilibrium structures to any other is given by the difference in energy between the two. While the gain in energy accompanied with the distortion from D_{nh} (where this total symmetry corresponds to a general radical $(CH)_n^{\cdot}$) to any of the predicted minima is not observable, the barriers of interconversion between the equivalent structures of all three mentioned cases have been estimated by ESR measurements. Figure 6 shows the predicted structures of the real minima and the saddle points. The calculated barriers of interconversions are given and compared with experiment in Table I.

While the calculated barriers are in striking agreement with experiment, the absolute values (ΔH_f) are somewhat in error.

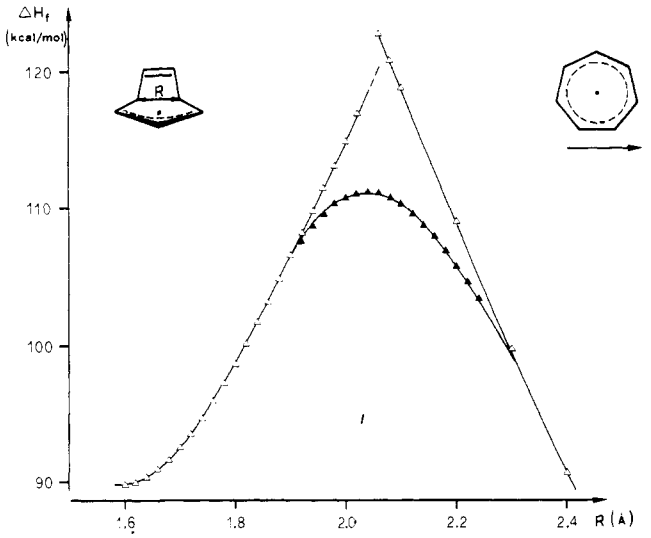

Figure 7. Calculated reaction profile for the disrotatory ring enlargement of bicyclo[3.2.0]heptatrienyl radical.

A vital question arises at this level: is there any general rule concerning the relative "aromaticities" of $4n + 1$ vs. $4n + 3$ radicals analogous to the well-known $4n + 2$ Hückel rule?

To investigate this, we have calculated the aromatic stabilization energies (ASE)[15] of the three key π radicals. To do so, one can compare the hydrogen atom affinities of the cyclic systems with those of the open chain analogues.

The results are summarized in Table II. Apparently, $(CH)_3$· is slightly "antiaromatic", while $(CH)_7$· is largely "aromatic". Both predictions have been confirmed by experimental studies.[16,17] Although both radicals are $4n + 3$ electron systems, the conjugation leads to opposite results concerning the aromatic stabilization energies.

These results illustrate again that a simple Hückel rule such as for closed shell systems is not at hand and that for the moment more elaborate calculations are needed.

Electrocyclic Rearrangement of Bicyclo[3.2.0]heptadienyl Radical. Encouraged by these results, we investigated the isomerization of bicyclo[3.2.0]heptadienyl radical (**4**) which has recently been studied experimentally.[18] As the reaction coordinate Q_1, the C^1C^5 bond was chosen. The calculated structure of the reactant **4** is shown below. MINDO/3-UHF

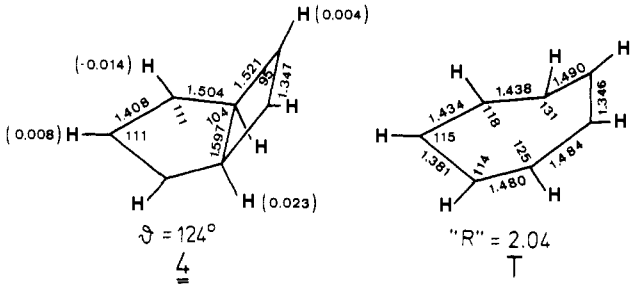

predicted the structure to have C_s symmetry with the five-membered ring being essentially planar. Our result clearly shows that the π-π interaction of the double bond with the allyl system is negligible and that the observed spin polarization toward the methylene protons in the four-membered ring is due to σ-π interaction of the cyclobutane Walsh orbitals[17] with the allyl π orbitals. The calculated spin densities (given in parentheses below) correlate reasonably well with the observed hyperfine coupling constants.

The calculated reaction profile is shown in Figure 7. Enforcing C_s symmetry, the energy raises steadily until self-consistency (R = 2.06 Å) was not achieved any more. A second run employed the independent optimization of the 41 geometrical variables. At a distance of R = 1.9 Å, the deviation from C_s symmetry became appreciable leading to the transition state T shown above. Checking the force constants revealed that just one of them was negative, indicating a true transition state. The calculation predicts an activation energy of 21.4 kcal/mol.

The measured *free* activation energy was found[18] to be 21.5 kcal/mol. Unfortunately, the temperature dependence of the reaction has not been published and the two values cannot of course be compared directly. The fact that the transition state is structurally close to the reactant **4** seems to indicate that the activation entropy $\Delta S^{\ddagger}$ should not be very large. Hence, the MINDO/3-UHF result—though possibly somewhat too low—is definitely in the right order.

Table II. Heats of Formation (ΔH_f), Hydrogen Atom Affinities (ΔH_H), and Aromatic Stabilization Energies (ASE) of Neutral Cyclic π Radicals (kcal/mol)

R·	ΔH_f	ΔH_H[a]	ASE[a]
Cyclopropenyl	96.8	89.5	−7.8
Allyl	36.1	81.7	
Cyclopentadienyl	66.8	77.2	−0.8
Pentadienyl	43.1	76.4	
Tropyl	47.8	62.6	+10.3
Heptatrienyl	52.0	72.9	

[a] Values calculated by thermocycle using the predicted heats of formation of the reactants in their optimized equilibrium geometries.

Conclusions

The MINDO/3-UHF calculations presented in this work clearly show that this method is capable of treating Jahn-Teller distorted radicals reasonably well, at least as far as the relative energies are concerned.

The close analogy between the potential surfaces of Jahn-Teller molecules and transition states and biradicaloid intermediates of forbidden reactions has been recognized by Dewar.[19] The present work shows that there is no principal difference between "forbidden" reactions no matter whether the total number of electrons is even or odd. However, while a closed shell system in most cases will find an "allowed" alternative course of reaction, the doublet system will have to follow the "less forbidden" path.

Qualitative as well as semiquantitative considerations indicate that no sound predictions can be made from frontier orbital considerations alone. If radical rearrangements occur stereospecifically at all, our method seems to be adequate in a predictive sense. However, the fact that such rearrangements can proceed via two equivalent transition states is a severe complication in the construction of reaction profiles. We share the opinion of others[21] that in cases where the stereochemical reaction path is questionable, these one-dimensional energy profiles are of little help and have to be accepted with caution.

References and Notes

(1) R. B. Woodward and R. Hoffmann, *Angew. Chem., Int. Ed. Engl.*, **8**, 781 (1969).
(2) The term "accidental degeneracy" is used to distinguish it from those cases where the symmetry of the system is responsible for the degeneracy.
(3) M. J. S. Dewar, *Angew. Chem., Int. Ed. Engl.*, **10**, 761 (1971).
(4) H. C. Longuet-Higgins and E. W. Abrahamson, *J. Am. Chem. Soc.*, **87**, 2045 (1965); N. L. Bauld and J. Cessac, *ibid.*, **99**, 23 (1977).
(5) N. Bauld, J. Cessac, C. S. Chang, F. R. Farr, and R. Holloway, *J. Am. Chem. Soc.*, **98**, 4561 (1976).
(6) M. J. S. Dewar, *Chem. Br.*, **11**, 97 (1975); M. J. S. Dewar, G. J. Fonken, S. Kirschner, and D. E. Minter, *J. Am. Chem. Soc.*, **97**, 6750 (1975); M. J. S.

Dewar and S. Kirschner, *ibid.*, **97**, 2932 (1975), and preceding papers of that series.
(7) L. Salem, C. Leforestier, G. Segal, and R. Wetmore, *J. Am. Chem. Soc.*, **97**, 479 (1975).
(8) R. C. Bingham, M. J. S. Dewar, and D. H. Lo, *J. Am. Chem. Soc.*, **97**, 1285 (1975); P. Bischof, *ibid.*, **98**, 6844 (1976).
(9) J. Pancir and R. Zahradnik, *Tetrahedron*, **32**, 2257 (1976).
(10) T.-K. Ha, F. Graf, and H. H. Günthard, *J. Mol. Struct.*, **15**, 335 (1973).
(11) N. C. Baird, *J. Org. Chem.*, **40**, 624 (1975).
(12) G. Cirelli, F. Graf, and H. H. Günthard, *Chem. Phys. Lett.*, **28**, 494 (1974).
(13) A. D. Baker, C. Baker, C. R. Brundle, and D. W. Turner, *Int. J. Mass Spectrom. Ion Phys.*, **1**, 285 (1968).
(14) E. Haselbach, *Chem. Phys. Lett.*, **7**, 428 (1970).
(15) M. J. S. Dewar, *Pure Appl. Chem.*, **44**, 767 (1975).
(16) K. Schreiner, W. Ahrens, and A. Berndt, *Angew. Chem., Int. Ed. Engl.*, **14**, 550 (1975).
(17) G. Vincow, H. J. Dauben, F. R. Hunter, and W. V. Volland, *J. Am. Chem. Soc.*, **91**, 2823 (1969).
(18) R. Sustmann and D. Brandes, *Tetrahedron Lett.*, 1791 (1976).
(19) M. J. S. Dewar and S. Kirschner, *J. Am. Chem. Soc.*, **96**, 5244 (1974).
(20) G. R. Liebling and H. M. McConnell, *J. Chem. Phys.*, **42**, 3931 (1965).
(21) A. Komornicki and J. W. McIver, Jr., *J. Am. Chem. Soc.*, **98**, 4553 (1976).
(22) H. J. Silverstone, D. E. Wood, and H. M. McConnell, *J. Chem. Phys.*, **41**, 2311 (1964).

Nuclear Magnetic Resonance Investigation of ^{15}N-Labeled Histidine in Aqueous Solution

F. Blomberg, W. Maurer, and H. Rüterjans*

Contribution from the Institute of Physical Chemistry, University of Münster, 4400 Münster, Germany. *Received April 11, 1977*

Abstract: The pH dependence of ^{15}N and ^{13}C resonances of histidine, 95% ^{15}N isotopically enriched in both imidazole nitrogens is studied. From the various couplings between the ^{13}C, ^{15}N, and ^{1}H nuclei a quantitative description of the tautomeric equilibrium of the deprotonated imidazole ring is possible. The chemical shift data and the coupling constants indicate an interaction of the α-amino group and the lone electron pair of the imidazole π nitrogen in the pH range of 6.2–9.3. Owing to this interaction the conformation of the whole molecule can be determined from the couplings. It can be shown that also the tautomeric equilibrium of the deprotonated imidazole is influenced by this interaction. The analysis of the pH dependence of the spin–lattice relaxation times T_1 and the NOE values reveals that histidine is associating around the pH value of the imidazole pK by forming possibly a dimeric structure.

In the last few years ^{15}N NMR spectroscopy has become a useful tool to investigate problems connected with the nitrogen atom in several organic molecules.[1-8] The low relative sensitivity compared to the ^{1}H NMR spectroscopy and the low natural abundance of the ^{15}N isotope can be overcome by NMR pulse techniques and/or large volume probes. The advantages of the method—large scale of chemical shifts, high sensitivity of the ^{15}N resonance to electronic and environmental effects—are promising also for the application in studying biological substances,[9-22] since nitrogen in the corresponding compounds is involved in many biological processes. For the investigation of biological molecules enrichment of the ^{15}N isotope seems necessary since in most cases there is not much material available.

In this paper we want to describe the behavior of histidine in aqueous solution using nitrogen-15 and carbon-13 NMR. Histidine is known to be part of the active site of many enzymes.[23] The imidazole ring often plays a role in the catalytic function of these enzymes. It was the aim of our investigation to study the structural features of the imidazole ring of histidine and its interaction with the solvent water.

Experimental Section

D,L-Histidine, ^{15}N isotope enriched in both nitrogen atoms of the imidazole ring (~95% ^{15}N), was purchased from Rohstoff-Einfuhr-GmbH, Düsseldorf, Germany.

NMR measurements were performed using 2 mL of an 0.2 M solution. For the determination of relaxation times T_1 and of NOE values, solutions free of paramagnetic impurities are needed. To remove traces of paramagnetic ions we have used the following procedures. D,L-Histidine was dissolved in an alkaline solution of doubly distilled H_2O and given to a small column of activated Chelex 100 (Biorad Laboratories, Richmond, Calif.). The elution from the column was carried out with doubly distilled H_2O and the amino acid lyophilized. After lyophilization the amino acid was again dissolved in H_2O which was extracted five times with a solution of dithizone in CCl_4 according to Pearson et al.[24] This solution was always freshly made and had a basic pH value due to the purification procedure which was carried out at high pH values. Therefore only the adjustment with a concentrated HCl solution to lower pH values was necessary.

All glassware, tubes, and plugs used in these procedures were soaked overnight in an alkaline solution of EDTA and rinsed thoroughly with doubly distilled water.

pH values were measured directly in the 10-mm NMR sample tube (Wilmad Glass Co., Buena, N.J.) using a special combined electrode (Ingold, Frankfurt, Germany) and a Radiometer pH meter (Model PHM 26).

All ^{15}N NMR measurements were performed on a Bruker HFX 90 at 9.12 MHz with Fourier transform mode employing a deuterium lock device. The deuterium signal was provided by D_2O in a coaxial capillary inside the 10-mm NMR sample tube.

The temperature was maintained with a Bruker temperature control unit BST 100/700 and determined to be 38 ± 2 °C. ^{13}C NMR measurements were carried out with a Bruker WH 270 at 67.89 MHz. The ^{15}N NMR relaxation times T_1 were determined by the inversion recovery method ($180°$-τ-$90°$-$5T_1$). Usually five scans were used to increase the signal-to-noise ratio. The T_1 values were calculated using a three-parameter nonlinear least-squares program according to the equation $M(\tau) = M_0(1 - ce^{-\tau/T_1})$.[25] The signal amplitudes were used as a probe for the magnetization $M(\tau)$. The NOE values were obtained from a comparison of spectra with and without proton broad band decoupling. The ratio of the integrated areas under the peaks was used to determine the NOE. Titration curves were calculated and fitted using the pH dependence of the chemical shift values (δ) or the coupling constants (J) according to the Henderson–Hasselbalch equation:

$$\delta_{obsd} = \delta_{min} + \sum_i \Delta\delta_i \frac{10^{pH-pK_i}}{1 + 10^{pH-pK_i}} \quad (1)$$

or

$$J_{obsd} = J_{min} + \sum_i \Delta J_i \frac{10^{pH-pK_i}}{1 + 10^{pH-pK_i}} \quad (2)$$

where δ_{min} = minimum value of the chemical shift, $\Delta\delta_i$ = difference